Energy and Momentum in Mechanical Impact Testing

Steven A. Mathe[1], Alfredo Juarez[1], and Stephen F. Peralta[2]

ABSTRACT

The ASTM G86 method is used to determine the ignition sensitivity of materials to mechanical impact in oxygen. It has long been known different systems built to the standard produce different results. Given the current push towards direct comparison of numerical results from different systems rather than just material rankings, it is desirable to normalize the systems to some performance-based metric. Normalization is complicated by the fact energy and momentum of a particular impact scale differently with plummet mass and drop height, and therefore adjusting the mass and height to account for system differences would result in a different impact. The standard uses dent blocks to assess impacts. However, it was unknown if the differences in momentum could be identified during dent block impacts. To determine this, dent blocks were impacted with constant energy and different momentums, using instrumented and non-instrumented plummets. The dent blocks showed statistically significant differences in the penetration function when subjected to impacts with the same energy but different momentum. Further, the instrumented plummet showed drastic differences in the power delivery with different momentums. System configuration was also shown to impact the response of the penetration function to different momentums.

[1] Sierra Lobo, Inc., NASA Materials and Laboratories Office, NASA Johnson Space Center White Sands Test Facility, P.O. Box 20, Las Cruces, NM 88004, USA
[2] NASA Materials and Laboratories Office, NASA Johnson Space Center White Sands Test Facility, P.O. Box 20, Las Cruces, NM 88004, USA

Keywords

Mechanical impact testing, ASTM G86, dent blocks, impact energy, impact momentum, impact power

Introduction

Drop-weight-based mechanical impact testers are commonly used to determine the sensitivity of reactive materials. [1-7] In these tests, a plummet of known mass is allowed to free-fall from a known height onto some intermediate body which transfers the energy from the plummet to the test sample resting on an anvil, with the sample then either reacting or not. These standards produce either a 50 % reaction value or a threshold value, reported in terms of either the drop height of the standard plummet or the nominal potential energy. These values are typically intended only to provide a relative measure of sensitivity to permit the materials under test to be ranked, with one standard version of the test going so far as to say the sensitivity values produced by the test are only defined in terms of the test.[3]

There is a push in the aerospace community to directly compare and make use of the numerical results obtained from different systems constructed in accordance with the ASTM G86-17, *Standard Test Method for Determining Ignition Sensitivity of Materials to Mechanical Impact in Ambient Liquid Oxygen and Pressurized Liquid and Gaseous Oxygen Environments* method. However, it has long been known different systems constructed per the ASTM G86 standard can produce widely varying threshold values for a given material, particularly when comparing systems intended for ambient pressure operation versus those intended for pressurized operation.[8] Therefore, it is desirable to normalize the results from each system in some fashion, under the assumption that differences in energy losses during the drop could be compensated for

by either a slight addition of drop mass or a slight increase in drop height. The first inclination is to normalize based on the impact energy—an approach which is used by at least three standard versions of impact testers to normalize results across different plummet masses, including an early description of the commonly used Army Ballistic Missile Agency (ABMA)-style impact system.[3,7,9]

Unfortunately, a simple analysis shows attempting to normalize impacts in this manner may not result in equivalent impacts. In drop-weight testing, the impact energy is ultimately derived from the potential energy of the plummet raised to a given height. Therefore, the impact energy is

$$E = PE = mgh \tag{1}$$

where:

E = the impact energy (J),

PE = the potential energy (J),

m = the mass of the plummet (kg),

g = the acceleration due to gravity (m/s^2), and

h = the initial height of the plummet (m).

At the point of impact, under the assumption of a frictionless fall and no other energy losses, all the potential energy has been converted to kinetic energy.

$$E = KE = \frac{1}{2}mv^2 \tag{2}$$

where:

KE = the kinetic energy of the plummet at impact (J), and

v = the velocity of the plummet at impact (m/s).

Because the plummet has both mass and velocity at the point of impact, it also has an impact momentum.

$$p = mv = m\sqrt{2gh} \tag{3}$$

where:

p = the momentum at impact (kg-m/s)

with the impact velocity calculated by combining equations (1) and (2). Assuming a perfectly inelastic impact of a plummet onto a sample resting upon a massive immobile anvil where the plummet does not bounce, the kinetic energy of the plummet is dissipated into the sample and at the same time an impulse is imparted into the sample due to the change in the plummet momentum.

It can be seen from equations (1) and (3) the energy and momentum scale differently with respect to plummet mass and drop height, given a constant energy. For example, take the situation of a plummet of mass m dropped from a height $2h$ (scenario 1), and a second plummet of mass $2m$ dropped from a height h (scenario 2). The impact energy is the same in both cases ($E_1 = mg(2h) = E_2 = (2m)gh$), but the impact momentum is different ($p_1 = 2m\sqrt{gh}$ vs. $p_2 = 2m\sqrt{2gh} = p_1\sqrt{2}$). The more massive plummet has more momentum at impact and thus imparts a larger impulse into a sample while having the same energy, which may have an effect on the ignition of materials. Therefore, attempts to adjust impacts to account for system losses based solely on the impact energy may not result in equivalent impacts due to differences in delivered impulse. At this point it is worth noting the ASTM G86-17 standard explicitly states that for the purposes of the standard, the impact energy requirements are not satisfied by non-standard plummet mass and drop height combinations.[1]

Approach

The ASTM G86-17 standard uses impacts against dent blocks to evaluate impact system performance.[1] However, it was unknown if the standardized dent block characterization method would be able to differentiate between the objectively different impacts of equivalent energy but different momentum. Therefore, dent block testing was performed at various combinations of plummet mass and drop height intended to obtain impacts at the same nominal energy levels but with different impact momentums as well as impacts at the same nominal impact momentum but with different impact energies. Except as described below, the testing was performed in accordance with ASTM G86-17.

Testing was broken into three phases, all performed at the White Sands Test Facility (WSTF): an instrumented phase (Phase 1), and two non-instrumented phases (Phase 2 and Phase 3). Phase 1 testing was performed using an instrumented impact test system, shown in Figure 1. The base consisted of a hardened anvil, on top of a plate of 300 series stainless steel, on top of a plate of carbon steel, over a large air space. A pneumatically-actuated plummet catcher system was utilized to prevent multiple impacts on the dent blocks. The impact test system also included an instrumented plummet nose to record other parameters of interest, such as the force vs. time trace, delivered energy, and impact duration. This system had available plummet masses of 6.781 kg, 13.590 kg, 24.331 kg, and 35.671 kg, with available drop heights from ~3.8 cm to ~102 cm. The combinations of energy and momentum achievable with this test system and the selected test points for Phase 1 are shown in Figure 2, with the selected test points further described in Table 1. This testing was performed at ambient temperature.

FIG. 1. The instrumented impact test system used during Phase 1.

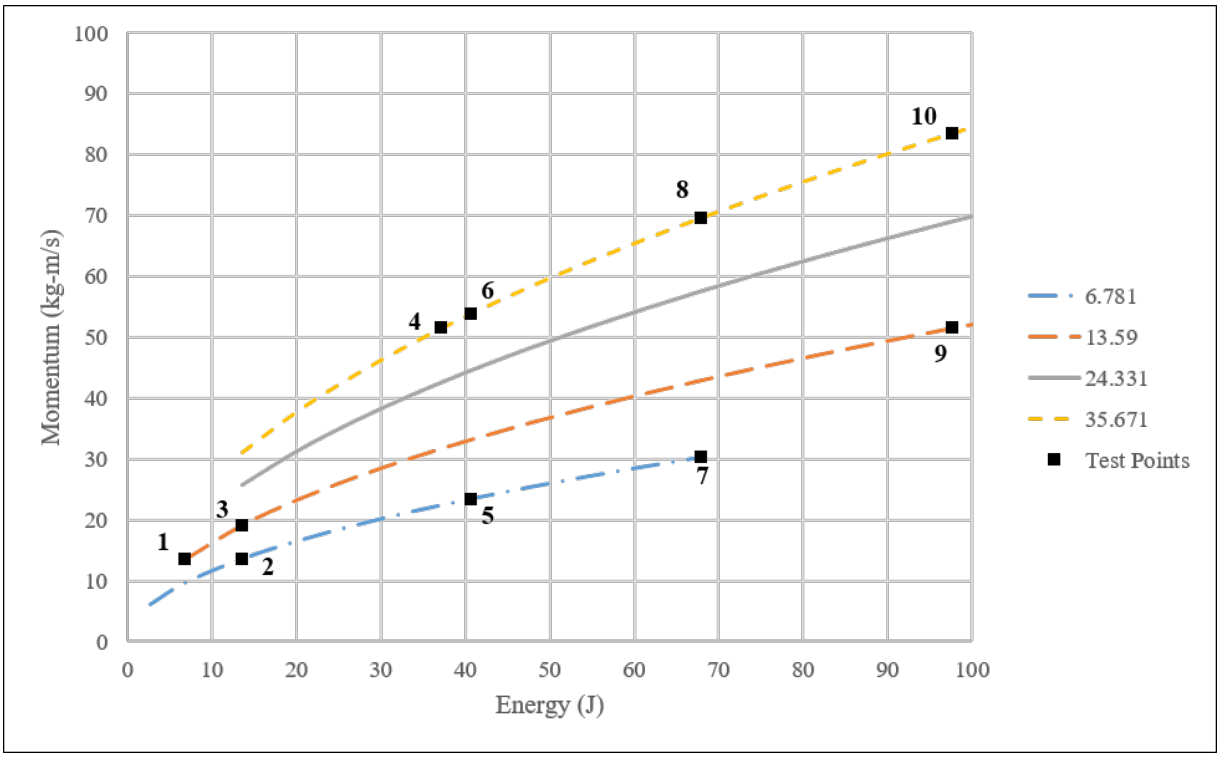

FIG. 2. The available test space in Phase 1. The legend indicates the mass of each plummet in kilograms.

TABLE 1 The selected test points for Phase 1.

Test Point	Nominal Energy (J)	Nominal Momentum at Impact (kg-m/s)	Plummet Mass (kg)	Drop Height (m)
1	6.78	13.6	13.59	0.051
2	13.6	13.6	6.781	0.204
3	13.6	19.2	13.59	0.102
4	37.1	51.5	35.671	0.106
5	40.7	23.5	6.781	0.612
6	40.7	53.9	35.671	0.116
7	67.8	30.3	6.781	1.02
8	67.8	69.5	35.671	0.194
9	97.6	51.5	13.59	0.732
10	97.6	83.5	35.671	0.279

Phase 2 testing was performed using the WSTF ABMA-style ambient pressure impact test system. The base consisted of a hardened anvil, on top of a block of 300 series stainless steel, on top of a block of concrete resting on the ground. A pneumatically-actuated plummet catcher system was utilized to prevent multiple impacts on the dent blocks. This system had available plummet masses of 2.275 kg and 9.068 kg, with available drop heights from ~7.6 cm to ~122 cm. The combinations of energy and momentum achievable with this test system and the selected test points for Phase 2 are shown in Figure 3, with the selected test points further described in Table 2. This testing was performed at ambient temperature.

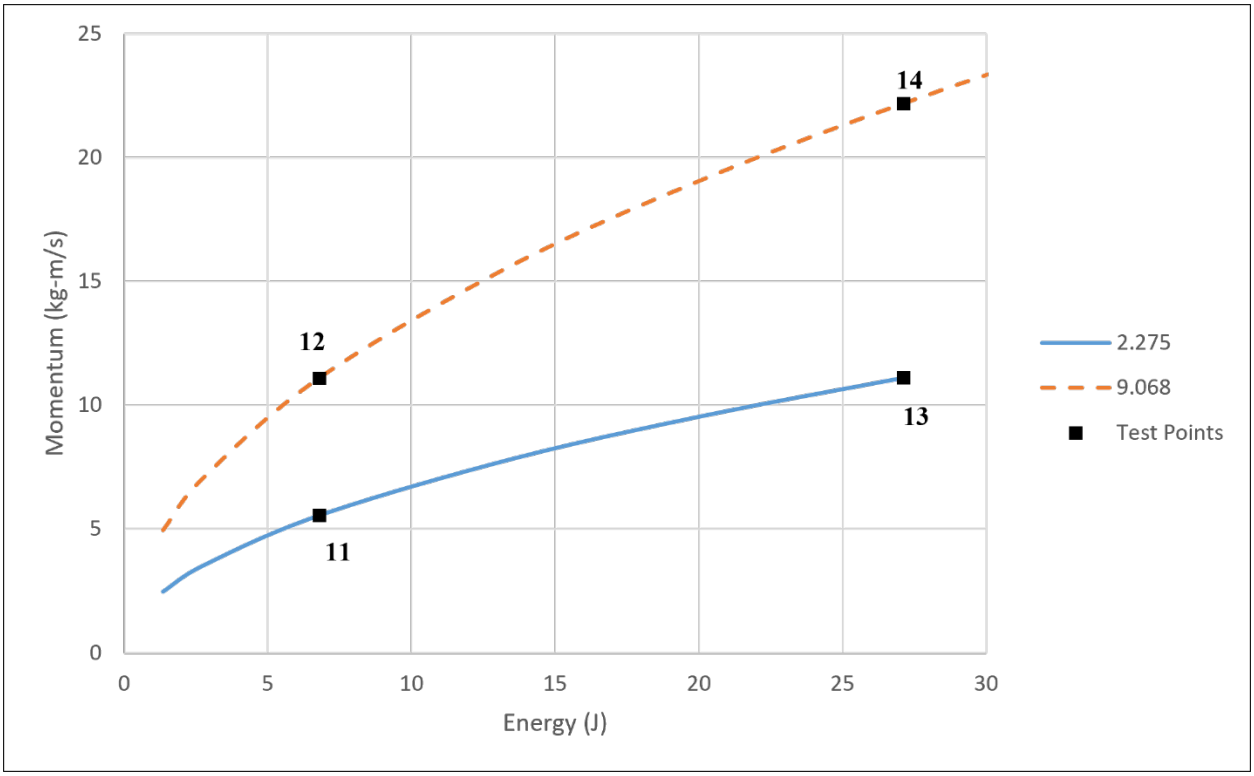

FIG. 3. The available test space in Phase 2. The legend indicates the mass of each plummet in kilograms.

TABLE 2 The selected test points for Phase 2.

Test Point	Nominal Energy (J)	Nominal Momentum at Impact (kg-m/s)	Plummet Mass (kg)	Drop Height (m)
11	6.78	5.55	2.275	0.304
12	6.78	11.1	9.068	0.076
13	27.1	11.1	2.275	1.22
14	27.1	22.2	9.068	0.305

Phase 3 testing was performed using the WSTF pressurized impact test system. The anvil consisted of a screw threaded into the test chamber, which is welded to the end of a stainless-steel pipe, on top of a stainless-steel block, on top of a block of concrete resting on the ground. A pneumatically-actuated plummet catcher system was utilized to prevent multiple impacts on the

dent blocks. From an energy/momentum standpoint, this system had the same available test space as the WSTF ABMA-style tester used in Phase 2 and the same test points were utilized. However, testing was performed at three pressures: ambient (0.087 MPa), 17.2 MPa, and 34.5 MPa. This testing was performed at ambient temperature.

Two dent block materials were used in this testing to observe any differences which may arise from using dent blocks of different hardness: annealed 304 stainless steel and hard 110 copper. All dent blocks were machined according to the dimensions listed in ASTM G86-17. The dent blocks did not undergo any heat treatment after machining. Hardness testing was performed on five dent blocks of each material. Both dent block materials were used in each phase of testing, with five tests of each material at all test points in Phases 1 and 2, and two tests each in Phase 3.

Results

Hardness testing was performed on five randomly selected samples each of both dent block materials. On each block, the hardness was tested at five locations in a line across the face of the block. The annealed 304 stainless-steel blocks had an average hardness value of 96.9 HRB (~217 HB), which is harder than the standard dent blocks (150 ± 15 HB). The stainless-steel blocks did exhibit signs of non-uniform hardness, with an average hardness of 91.6 HRB in the middle of the block face and an average hardness of 100 HRB near the edges of the block face. The hard 110 copper blocks had an average hardness value of 41.1 HRB, which was fairly uniform across all sample locations.

Because of a failure in the test system, only a partial Phase 1 test matrix was completed. Table 3 shows the summarized results including only the data points which provide direct

comparisons between equivalent energies but different momentums. The plot of penetration function vs. measured impact energy is shown in Figure 4 and includes all Phase 1 data points. Figure 5 shows the plot of penetration depth vs. measured impact momentum and Figure 6 shows the plot of penetration function vs. average power, both with all Phase 1 data points.

TABLE 3 Summarized results from Phase 1, containing only the equivalent energy pairs.

Test Point	7	8	5	6	7	8
Material	Cu	Cu	SS	SS	SS	SS
Number of Tests	1	2	3	5	2	4
Impact Velocity (m/s)	4.42	1.93	3.41	1.49	4.45	1.92
Impact Duration (ms)	1.25	3.09	0.96	2.50	0.95	2.45
Measured Impact Energy (J)	65.9	66.4	36.5	37.9	62.7	63.3
P-Value Comparing Energy	0.253		0.022		0.486	
Measured Momentum at Impact (kg-m/s)	30.0	68.8	23.1	53.1	30.2	68.6
Average Power (kW)	52.7	21.5	38.0	15.2	38.1	25.8
P-Value Comparing Power	0.0095		2.33e-7		5.96e-7	
Ave. Pen. Depth (mm)	1.5884	1.5098	0.6584	0.5928	0.8541	0.7584
Ave. Pen. Function (mm^2)	2.5260	2.2797	0.4338	0.3516	0.7295	0.5752
P-Value Comparing Pen. Function	0.0721		0.0012		0.0008	

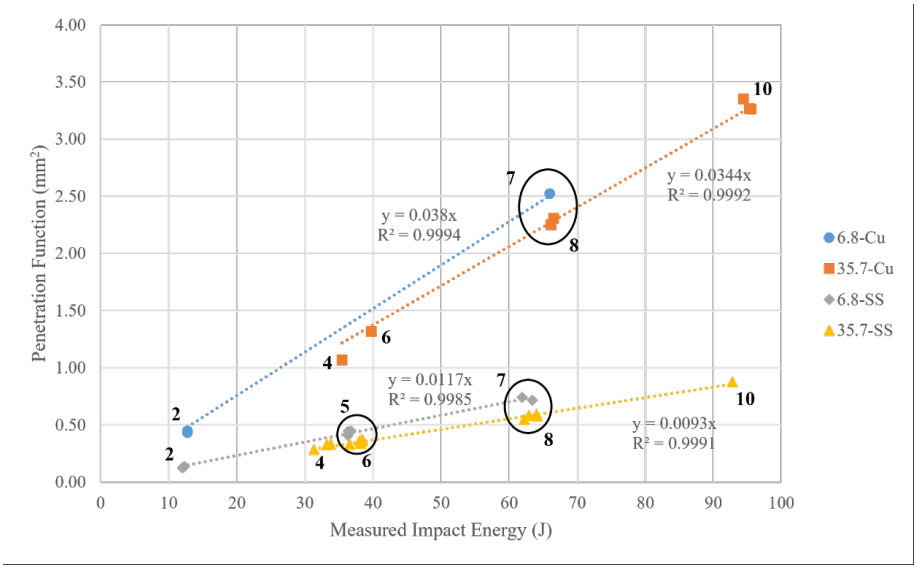

FIG. 4. Phase 1 penetration function vs. measured impact energy. Equivalent energy pairs are circled. The bold numbers refer to the energy/momentum test points shown in Figure 2. The legend indicates the plummet mass in kilograms and the material of the dent blocks. Equation fits were forced through the origin in keeping with the practice of ASTM G86.[1]

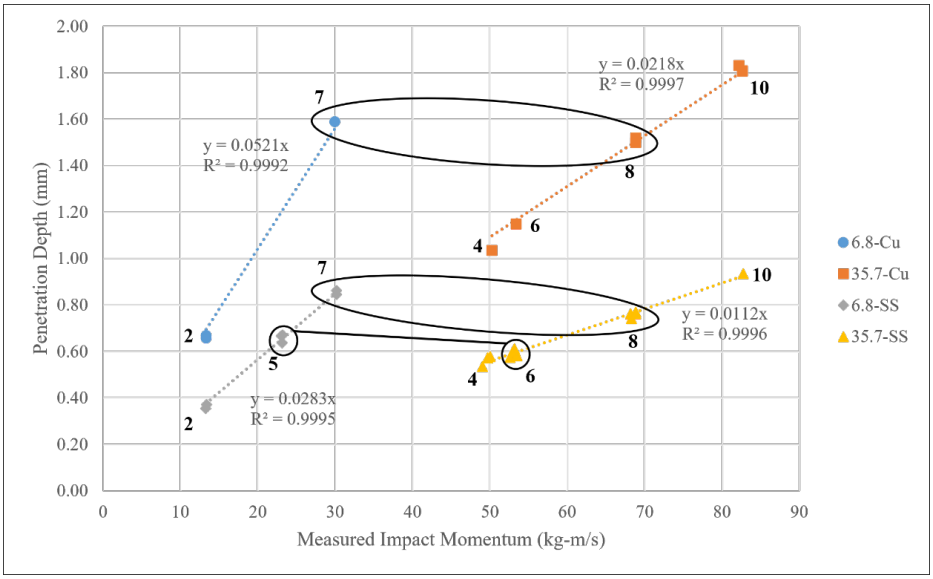

FIG. 5. Phase 1 penetration depth vs. measured plummet momentum at impact. Equivalent energy pairs are circled. The bold numbers refer to the energy/momentum test points shown in Figure 2. The legend indicates the plummet mass in kilograms and the dent block material. Equation fits were forced through the origin in keeping with the practice of ASTM G86.[1]

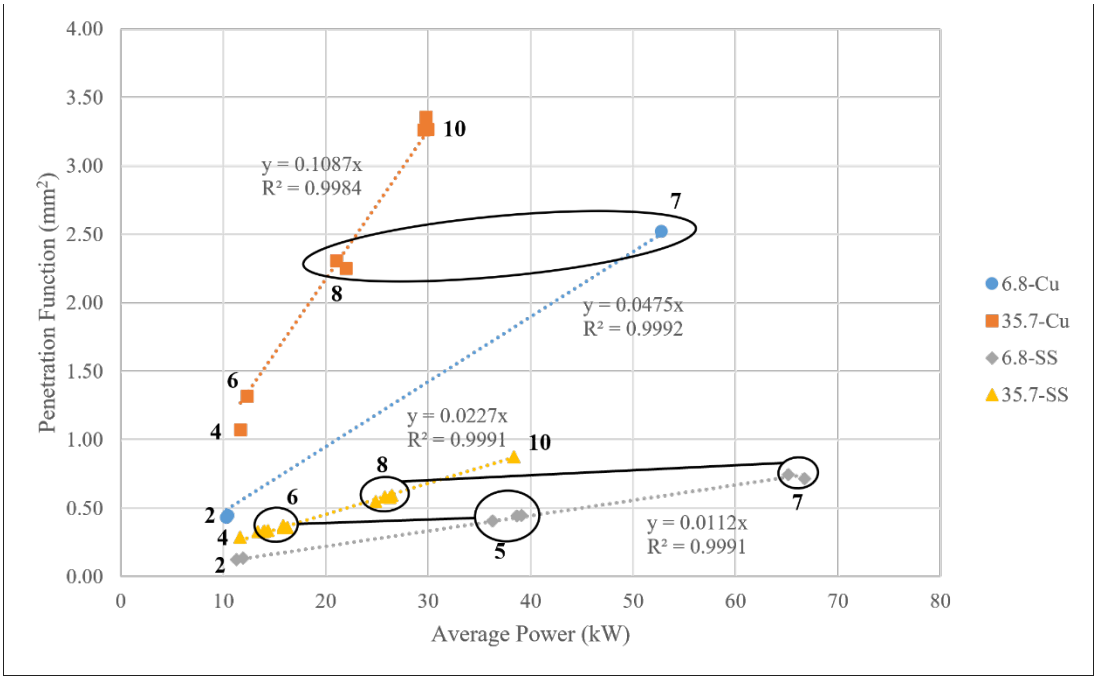

FIG. 6. Phase 1 penetration function vs. average power. Equivalent energy pairs are circled. The bold numbers refer to the energy/momentum test points shown in Figure 2. The legend indicates the plummet mass in kilograms and the dent block material. Equation fits were forced through the origin in keeping with the practice of ASTM G86.[1]

The Phase 2 test matrix was completed as planned. The summarized results are shown in Table 4. Figure 7 shows the plot of penetration function vs. nominal impact energy while Figure 8 shows the plot of penetration depth vs. nominal impact momentum.

TABLE 4 Summarized results from Phase 2.

Nominal Energy (J)	Nominal Momentum (kg-m/s)	Plummet Mass (kg)	Material	Ave. Pen. Depth (mm)	Ave. Pen. Function (mm²)	P-Value
6.78	5.55	2.275	Cu	0.4682	0.2193	7.77e-6
6.78	11.09	9.068	Cu	0.5273	0.2782	
27.12	11.11	2.275	Cu	0.9885	0.9774	2.31e-5
27.12	22.18	9.068	Cu	1.0783	1.1632	
6.78	5.55	2.275	SS	0.2659	0.0707	2.62e-6
6.78	11.09	9.068	SS	0.3139	0.0986	
27.12	11.11	2.275	SS	0.5333	0.2845	1.25e-7
27.12	22.18	9.068	SS	0.6128	0.3757	

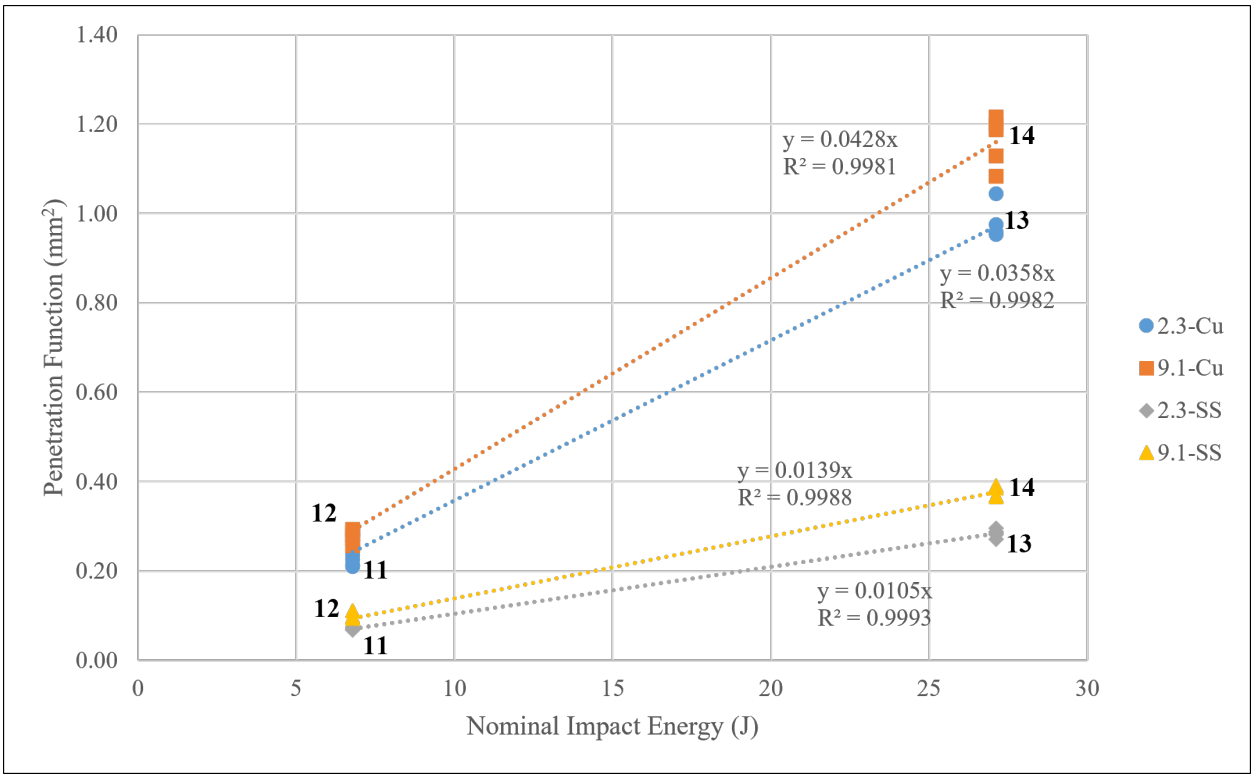

FIG. 7. Phase 2 penetration function vs. nominal impact energy. The bold numbers refer to the energy/momentum test points shown in Figure 3. The legend indicates the plummet mass in kilograms and the dent block material. Equation fits were forced through the origin in keeping with the practice of ASTM G86.[1]

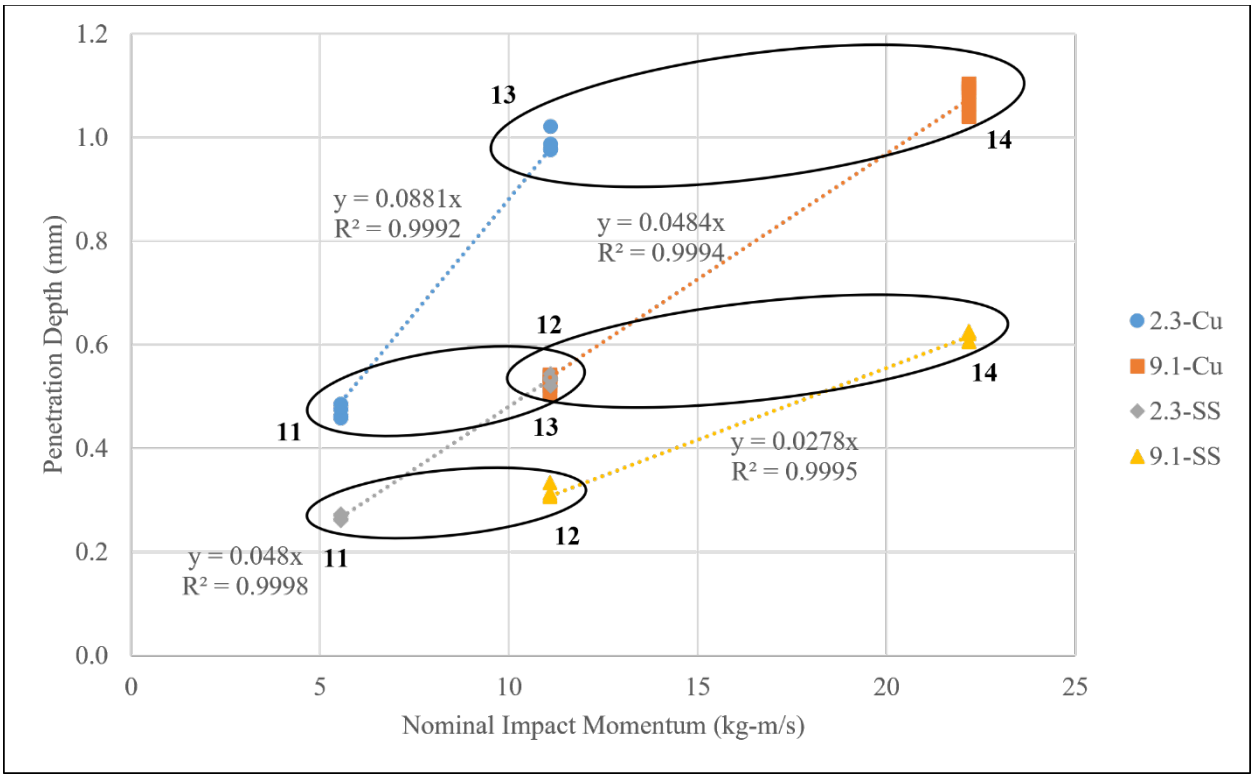

FIG. 8. Phase 2 penetration depth vs. nominal plummet momentum at impact. The equivalent energy pairs are circled. The bold numbers refer to the energy/momentum test points shown in Figure 3. The legend indicates the plummet mass in kilograms and dent block material. Equation fits were forced through the origin in keeping with the practice of ASTM G86.[1]

The Phase 3 test matrix was completed as planned. The summarized results are shown in Table 5. The results for the copper dent blocks are shown in Figures 9 and 10, which are the plot of penetration function vs. nominal impact energy and the plot of penetration depth vs. nominal impact momentum, respectively, while Figures 11 and 12 show the same for the stainless-steel dent blocks.

TABLE 5 Summarized Phase 3 results.

Nominal Energy (J)	Nominal Momentum (kg-m/s)	Plummet Mass (kg)	Material	Chamber Pressure (MPa)	Ave. Pen. Depth (mm)	Ave. Pen. Function (mm^2)	P-Value Comparing Pen. Function
6.78	5.55	2.275	Cu	0.087	0.3997	0.1598	0.027
6.78	11.1	9.068	Cu	0.087	0.3937	0.1550	
27.1	11.1	2.275	Cu	0.087	0.8457	0.7152	0.277
27.1	22.2	9.068	Cu	0.087	0.8689	0.7551	
6.78	5.55	2.275	Cu	17.2	0.3935	0.1548	0.020
6.78	11.1	9.068	Cu	17.2	0.4171	0.1740	
27.1	11.1	2.275	Cu	17.2	0.6796	0.4782	0.171
27.1	22.2	9.068	Cu	17.2	0.9180	0.8426	
6.78	5.55	2.275	Cu	34.5	0.3012	0.0908	0.644
6.78	11.1	9.068	Cu	34.5	0.2952	0.0872	
27.1	11.1	2.275	Cu	34.5	0.7752	0.6011	0.072
27.1	22.2	9.068	Cu	34.5	0.8253	0.6813	
6.78	5.55	2.275	SS	0.087	0.2122	0.0450	0.089
6.78	11.1	9.068	SS	0.087	0.2052	0.0421	
27.1	11.1	2.275	SS	0.087	0.4300	0.1849	0.156
27.1	22.2	9.068	SS	0.087	0.4170	0.1739	
6.78	5.55	2.275	SS	17.2	0.1977	0.0391	0.089
6.78	11.1	9.068	SS	17.2	0.2153	0.0464	
27.1	11.1	2.275	SS	17.2	0.2711	0.0735	3.71e-5
27.1	22.2	9.068	SS	17.2	0.4372	0.1912	
6.78	5.55	2.275	SS	34.5	0.1741	0.0304	0.469
6.78	11.1	9.068	SS	34.5	0.1634	0.0267	
27.1	11.1	2.275	SS	34.5	0.3662	0.1341	0.120
27.1	22.2	9.068	SS	34.5	0.3912	0.1531	

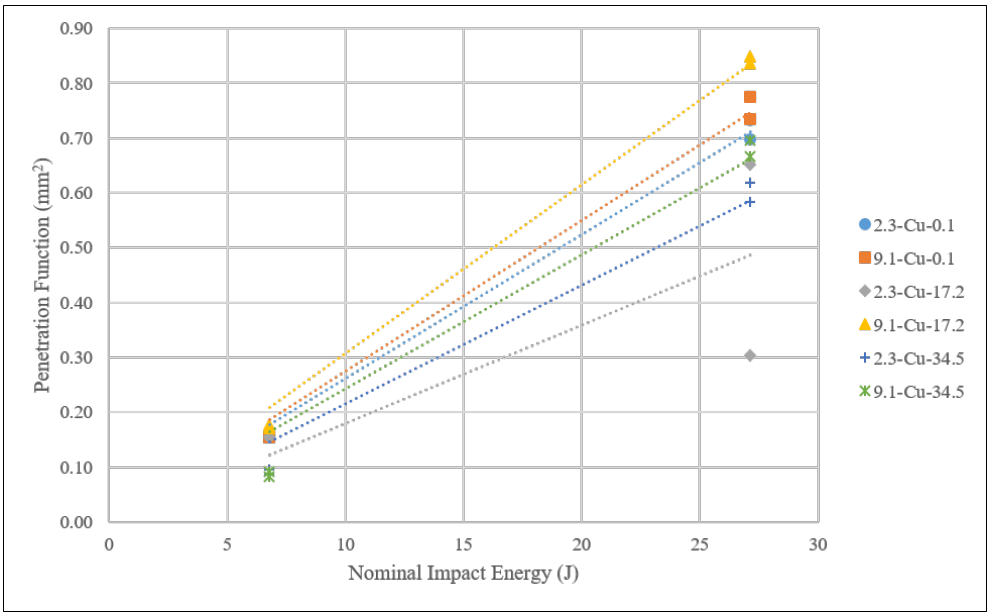

FIG. 9. Phase 3 penetration function vs. nominal impact energy for the copper dent blocks. The legend indicates the plummet mass in kilograms, dent block material, and chamber pressure in MPa. Equation fits were forced through the origin in keeping with the practice of ASTM G86.[1]

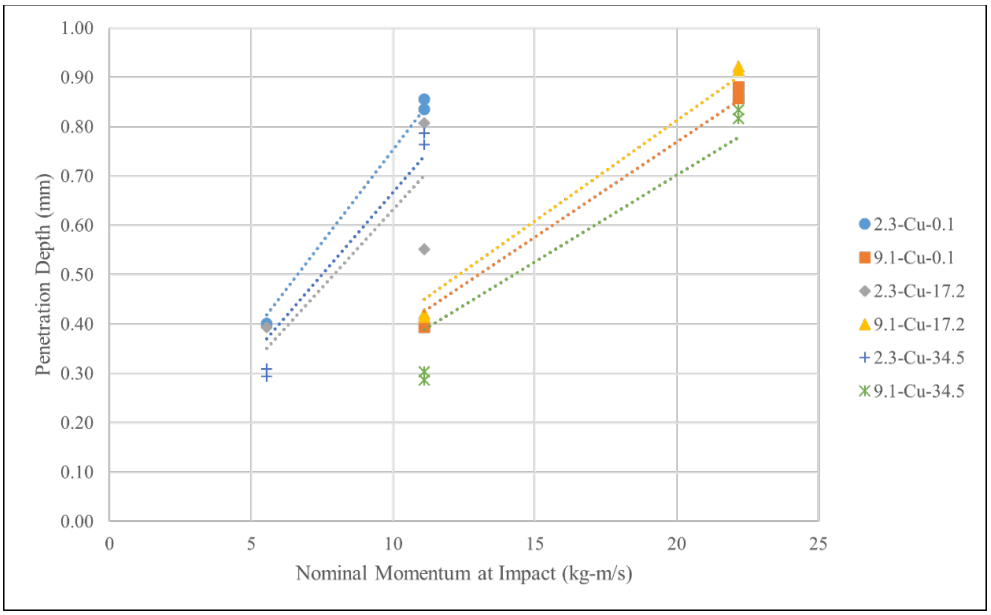

FIG. 10. Phase 3 penetration depth vs. nominal plummet momentum at impact for the copper dent blocks. The legend indicates the plummet mass in kilograms, dent block material, and chamber pressure in MPa. Equation fits were forced through the origin in keeping with the practice of ASTM G86.[1]

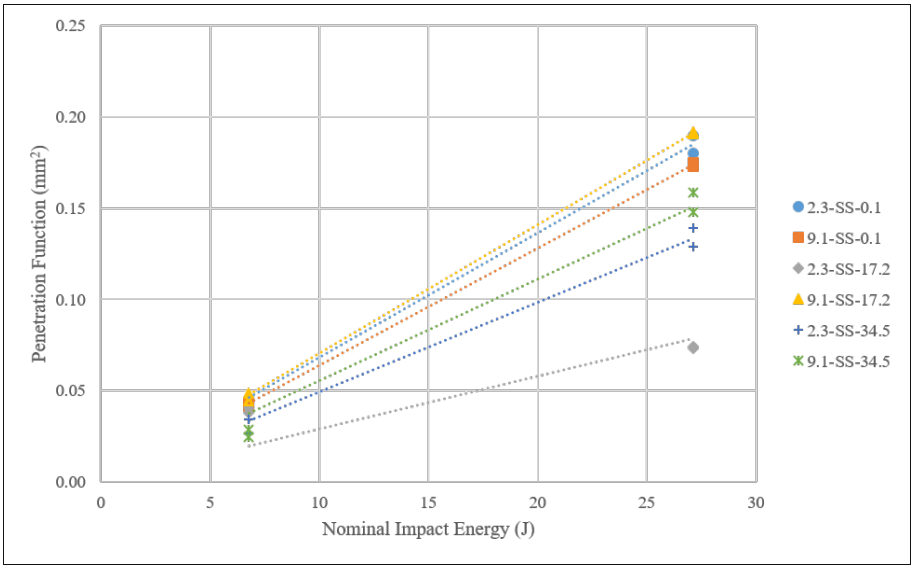

FIG. 11. Phase 3 penetration function vs. nominal impact energy for the stainless-steel dent blocks. The legend indicates the plummet mass in kilograms, dent block material, and chamber pressure in MPa. Equation fits were forced through the origin in keeping with the practice of ASTM G86.[1]

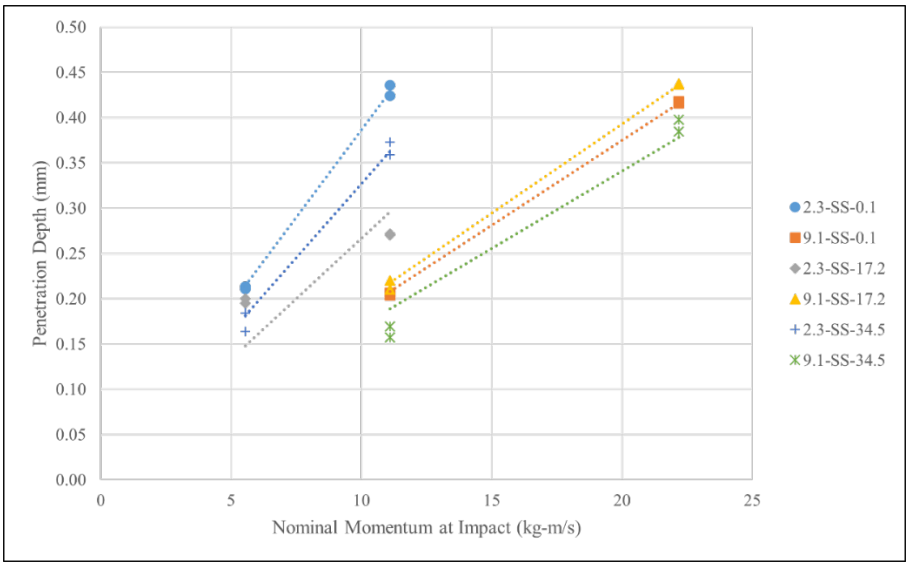

FIG. 12. Phase 3 penetration depth vs. nominal plummet momentum at impact for the stainless-steel dent blocks. The legend indicates the plummet mass in kilograms, dent block material, and chamber pressure in MPa. Equation fits were forced through the origin in keeping with the practice of ASTM G86.[1]

Discussion

The instrumented impact system used in the Phase 1 testing was able to measure the impact energy for each impact at the plummet nose. Of the Phase 1 datasets with nominally equivalent energies produced through drops of different mass plummets, two of the three sets indicated no significant difference in the energy delivery, indicating this testing was successful in producing impacts of equivalent energy. One set (40.7 J nominal impact energy into stainless-steel dent blocks) did show a somewhat significant difference in the energy delivered by the different mass plummets, at the $\alpha = 0.05$ level using a two-tailed Student's *t*-test. Given that this pair included the largest number of data points in Phase 1 (eight data points between the two plummet masses), it is suspected the impact energy may have been different, possibly due to slight variations in the actual drop height. Because the systems used in Phases 2 and 3 did not have an instrumented plummet, it is not possible to calculate the actual energy delivery and it will be assumed there was effectively no difference in the energy delivered by either plummet at a given nominal energy level.

Looking at the Phase 1 dent block data, statistically significant differences at the $\alpha = 0.05$ level using a two-tailed Student's *t*-test were observed in the penetration function for two of the three equivalent energy pairs. In the pair that was not significant (67.8 J nominal impact energy into copper dent blocks), it is suspected this is due to the low number of test points (one with the 6.78 kg plummet and two with the 35.67 kg plummet) and the accompanying wide statistical bands. In all three cases, the trend was that the lighter plummet produced the larger dents at a given energy, as can be seen in Figure 4. Stated in another way, the Phase 1 data indicated increasing the momentum for a given impact energy actually resulted in smaller dents, which can be seen in Figure 5. This result was counter to the predictions of the test

team; however, a possible explanation was found in light of the Phase 2/3 data and will be discussed below. Upon further examination of Figures 4 and 5, it can be observed the plummet momentum at impact had a weak effect on the dent size relative to that of the impact energy, because for a given energy a ~130 % increase in plummet momentum only resulted in a ~7 % decrease in penetration depth and thus ~15 % decrease in penetration function. Unfortunately, due to the abbreviated test matrix no equivalent momentum pairs were tested so this comparison cannot be directly repeated in the case of a given momentum using the Phase 1 data.

The instrumented plummet offered the ability to examine other data relevant to the impact, most interestingly the average power of each impact. In all three of the equivalent energy pairs, statistically significant differences at the $\alpha = 0.05$ level using a two-tailed Student's *t*-test were observed in the average power. As can be seen from Figure 6, the trend for power was that an increase in power for a given energy resulted in an increased dent size in terms of penetration function, with the lighter plummet exhibiting higher power impacts. The difference in power is a manifestation of the fact that for the lighter plummet to have the same kinetic energy as a heavier one, it must be moving faster and thus the impact must happen faster delivering equivalent energy in a shorter time. It can also be observed from Figures 5 and 6 the strength of the influence of power on dent size matches the limited influence of plummet momentum.

Considering the purpose of the ASTM G86 standard, the small difference in response of the dent blocks at equivalent energies to different powers is potentially problematic. By changing the relationship between the impact energy and plummet momentum for a given drop by using different plummet masses and drop heights, the power of the impact is also changed. Further, it appears this change in power is something that may not be captured adequately by the dent block method currently used to assess the performance of ASTM G86 impact testers. It is well known

in the explosives field that the power of an initiation source matters in addition to the energy.[10] Previous impact testing in liquid oxygen using different mass plummets has shown differences in material reactivity.[9] The idea of incorporating a power assessment into mechanical impact testing is not new.[11] The Phase 1 results only serve to reinforce that idea.

Looking at the Phase 2 data, statistically significant differences at the $\alpha = 0.05$ level using a two-tailed Student's *t*-test were observed in the penetration function for all four of the equivalent energy pairs. Looking at Figure 7, the trend in all four pairs is the heavier plummet produced a larger dent for equivalent energy. Stated another way, adding momentum increased the dent size as shown in Figure 8. This trend is opposite that observed in the Phase 1 testing. Considering this trend reversal in light of the two systems used to collect the data, it was observed that the Phase 1 instrumented system was subjectively much less rigid than the Phase 2 ABMA-style system; the Phase 1 system has the impact tester directly over a large air space whereas the ABMA-style tester is mounted directly to a concrete block on the ground. The lighter plummets must also be moving faster to have the same kinetic energy as the heavier plummets, which has the side effect of decreasing the impact duration. This also decreases the time available for the structure of the impact tester to respond to an impact. Therefore, the subjectively more flexible structure of the Phase 1 tester does not have time to react to the faster impact from the lighter plummet but can flex and absorb impact energy on the longer timescale of the heavier plummet. With the Phase 2 ABMA-style tester, the subjectively more rigid structure does not react to the impact on either timescale allowing the extra momentum from the heavier plummet to produce a larger dent. This suggests system rigidity may be a further complicating factor in attempting interpret normalized impacts.

With respect to the strength of the relationship between energy and momentum on the dent size, the Phase 2 data produced a similar pattern as Phase 1. In this case, at a given energy a ~100 % increase in the plummet momentum produced only a ~14 % increase in penetration depth and thus ~30 % increase in penetration function. The Phase 2 data did include two equivalent momentum pairs, where a ~300 % increase in impact energy produced a ~79 % increase in penetration depth and thus ~220 % increase in penetration function.

In the Phase 3 testing, statistically significant differences at the $\alpha = 0.05$ level using a two-tailed Student's *t*-test were observed in the penetration function for only three of the 12 equivalent energy, equivalent pressure pairs. It is possible this is due simply to the fact only two tests were performed at each test point, but the trends exhibited by the significant pairs complicate that discussion. Of the three significant pairs, increased momentum produced a larger dent in two of the pairs while in the third it produced a smaller dent. Subjectively, the Phase 3 test system lies between the Phase 1 and 2 systems in terms of rigidity. It is suspected the Phase 3 system was coincidentally just flexible enough to absorb some energy from the heavier plummet impacts but less so than the Phase 1 system such that the dent sizes were broadly similar between the two plummets. Under this interpretation, more testing with the Phase 3 system would not be expected to increase the significance of difference between the dents produced by the different mass plummets. This further reinforces the idea system rigidity is a complicating factor in normalization. In addition, the low significance of momentum with respect to dent size in this phase of testing continues the trend from Phases 1 and 2.

Regarding the different material dent blocks, in terms of percentage difference, the observed trends were highly similar across all three phases of testing. However, the softer copper dent blocks exhibited physically larger dents for a given impact than the harder stainless steel.

Because of the physical size difference in dent size, the softer blocks may be capable of identifying smaller differences in a statistically significant manner.

Conclusion and Future Work

Industry is pushing to use mechanical impact testing in a numerical way despite the fact the tests were originally intended to produce relative rankings. Because of this, it is desired to normalize the impacts from different systems. However, the impact energy and the plummet momentum at impact scale differently from each other with respect to plummet mass and drop height. It was unknown how the ASTM G86 dent block calibration method would be able to distinguish between objectively different impacts of equivalent energy but different momentum.

Three phases of dent block testing similar to that described in ASTM G86 was performed using different mass plummets to produce equivalent energy impacts. Based on data collected from the instrumented plummet used in Phase 1, the different plummet masses were in fact capable of delivering equivalent energy impacts. In Phase 1 the higher momentum impacts for a given energy were found to produce smaller dents, while in Phase 2 the higher momentum impacts for a given energy were found to produce larger dents. Phase 3 found no particular trend between the momentum at a given energy and the dent size. Taken collectively, it is believed this is related to the flexibility of each impact system, where the slower impacts produced by the larger mass plummets allowed a flexible system to react and absorb some of the impact energy. Therefore, system rigidity may be a complicating factor in attempting to interpret normalized impacts, particularly when comparing between ambient pressure and pressurized test systems, or with systems not in strict keeping with ASTM G86.

In all three phases, momentum was found to have a weak effect on the dent size relative to the nominal impact energy, indicating the dent block method may have a poor ability to differentiate equivalent energy impacts based on momentum. Based on the data collected in Phase 1, the power of a particular impact had a similarly weak effect on the dent size. However, the power is known to have a strong influence on the reactivity of a material under test. Therefore, the dent blocks may not be an adequate method of characterizing the performance of the mechanical impact test system.

Two different dent block materials were utilized in this testing. The trends identified above were consistent across both materials, including similar differences on a percentage basis. However, because the softer copper dent blocks exhibited physically larger dents than the harder stainless steel dent blocks for a given impact, it is possible smaller percentage differences could be identified in a statistically significant way using the softer blocks.

The differences in impacts used in this study were more extreme than would be encountered in any actual normalization scenario, particularly considering the ASTM G86-17 prohibition on non-standard plummet masses. Future work would attempt to replicate a normalization scenario by introducing controlled losses into the system and then attempting to compensate, with impacts instrumented to provide a complete picture. Then the controlled loss system could be used with a real material in oxygen, to assess the effects of normalization attempts on reactivity.

ACKNOWLEDGMENTS

The authors would like to acknowledge the contributions of Susana A. Harper, Gabriel Favela, and John Bouvet in their efforts to produce the test data, and of April Vise in her efforts to edit this paper.

References

1. *Standard Test Method for Determining Ignition Sensitivity of Materials to Mechanical Impact in Ambient Liquid Oxygen and Pressurized Liquid and Gaseous Oxygen Environments*, ASTM G86-17 (West Conshohocken, PA: ASTM International, approved December 1, 2017). https://doi.org/10.1520/G0086-17.

2. *Standard Test Method for Compatibility of Materials with Liquid Oxygen (Impact Sensitivity Threshold and Pass-Fail Techniques)*, ASTM D2512-17 (West Conshohocken, PA: ASTM International, approved July 1, 2017). https://doi.org/10.1520/D2512-17.
3. *Standard Test Method for Drop-Weight Sensitivity of Liquid Monopropellants*, ASTM D2540-93(2001) (West Conshohocken, PA: ASTM International, withdrawn 2003). https://doi.org/10.1520/D2540-93R01.

4. *Standard Test Method for Drop Weight Impact Sensitivity of Solid-Phase Hazardous Materials*, ASTM E680-79(2018) (West Conshohocken, PA: ASTM International, approved November 15, 2018). https://doi.org/10.1520/E0680-79R18.

5. *Standard Test Method for Compatibility of Materials with Liquid Oxygen (Reaction Intensity Method)*, ASTM F371-83(1994) e1 (West Conshohocken, PA: ASTM International, withdrawn 2003). https://doi.org/10.1520/F0371-83R94E01.

6. *Standard Practice for Compatibility of Materials with High-Energy Propellants (Impact Sensitivity Threshold Technique)*, ASTM F764-82(1994) (West Conshohocken, PA: ASTM International, withdrawn 2003). https://doi.org/10.1520/F0764-82R94.

7. *Explosives, Impact Sensitivity Tests*, NATO STANAG 4489 (Edition 1) (Brussels, Belgium: NATO Standardization Office, amended September 20, 2013).

8. J. W. Bransford, C. J. Bryan, G. W. Frye, and S. L. Stohler, "Lox/Gox Mechanical Impact Tester Assessment," Technical Memorandum TM-74106, NASA, Washington, D.C., 1980.

9. W. R. Lucas, and W. A. Riehl, "An Instrument for Determination of Impact Sensitivity of Materials in Contact with Liquid Oxygen," ASTM Bulletin, ASTBA, No. 244, Feb. 1960, pp. 29-34.

10. P. W. Cooper, *Explosives Engineering* (Hoboken, NJ: Wiley-VCH, 1996), pp. 329-333.

11. D. Smith and R. H. Richardson, "Interpretation of Impact Sensitivity Test Data," *Pyrodynamics*, Vol. 6, (1968): pp. 159-178.

List of Figure Captions

FIG 1. The instrumented impact test system used during Phase 1.

FIG. 2. The available test space in Phase 1. The legend indicates the mass of each plummet in kilograms.

FIG. 3. The available test space in Phase 2. The legend indicates the mass of each plummet in kilograms.

FIG. 4. Phase 1 penetration function vs. measured impact energy. Equivalent energy pairs are circled. The bold numbers refer to the energy/momentum test points shown in Figure 2. The legend indicates the plummet mass in kilograms and the material of the dent blocks. Equation fits were forced through the origin in keeping with the practice of ASTM G86.[1]

FIG. 5. Phase 1 penetration depth vs. measured plummet momentum at impact. Equivalent energy pairs are circled. The bold numbers refer to the energy/momentum test points shown in Figure 2. The legend indicates the plummet mass in kilograms and the dent block material. Equation fits were forced through the origin in keeping with the practice of ASTM G86.[1]

FIG. 6. Phase 1 penetration function vs. average power. Equivalent energy pairs are circled. The bold numbers refer to the energy/momentum test points shown in Figure 2. The legend indicates the plummet mass in kilograms and the dent block material. Equation fits were forced through the origin in keeping with the practice of ASTM G86.[1]

FIG. 7. Phase 2 penetration function vs. nominal impact energy. The bold numbers refer to the energy/momentum test points shown in Figure 3. The legend indicates the plummet mass in kilograms and the dent block material. Equation fits were forced through the origin in keeping with the practice of ASTM G86.[1]

FIG. 8. Phase 2 penetration depth vs. nominal plummet momentum at impact. The equivalent energy pairs are circled. The bold numbers refer to the energy/momentum test points shown in Figure 3. The legend indicates the plummet mass in kilograms and dent block material. Equation fits were forced through the origin in keeping with the practice of ASTM G86.[1]

FIG. 9. Phase 3 penetration function vs. nominal impact energy for the copper dent blocks. The legend indicates the plummet mass in kilograms, dent block material, and chamber pressure in MPa. Equation fits were forced through the origin in keeping with the practice of ASTM G86.[1]

FIG. 10. Phase 3 penetration depth vs. nominal plummet momentum at impact for the copper dent blocks. The legend indicates the plummet mass in kilograms, dent block material, and chamber pressure in MPa. Equation fits were forced through the origin in keeping with the practice of ASTM G86.[1]

FIG. 11. Phase 3 penetration function vs. nominal impact energy for the stainless-steel dent blocks. The legend indicates the plummet mass in kilograms, dent block material, and chamber pressure in MPa. Equation fits were forced through the origin in keeping with the practice of ASTM G86.[1]

FIG. 12. Phase 3 penetration depth vs. nominal plummet momentum at impact for the stainless-steel dent blocks. The legend indicates the plummet mass in kilograms, dent block material, and chamber pressure in MPa. Equation fits were forced through the origin in keeping with the practice of ASTM G86.[1]